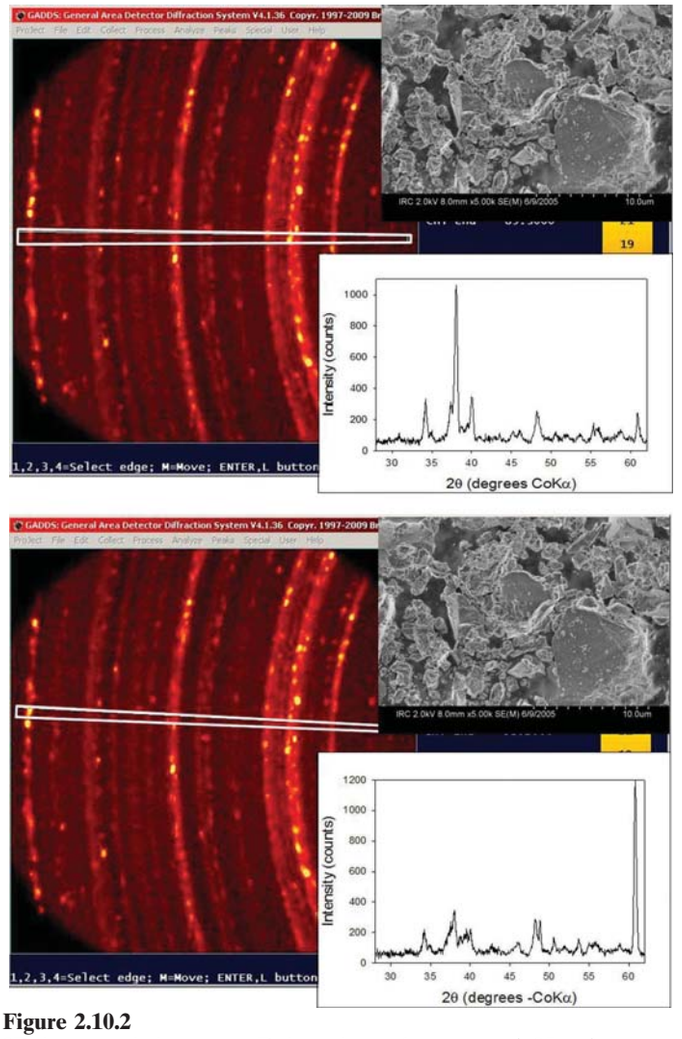

Figure 2.10.2
2D images of the spotty Debye rings of a coarse (~35 µm) cement powder using a Co *Kα* radiation 1 mm point source. Overlaid are SEMs of the sample material and integrated patterns from the thin slices indicated in the 2D patterns to illustrate what a point or 1D detector would see. Note: in these 2D data sets the low 2θ rings are on the right-hand side.

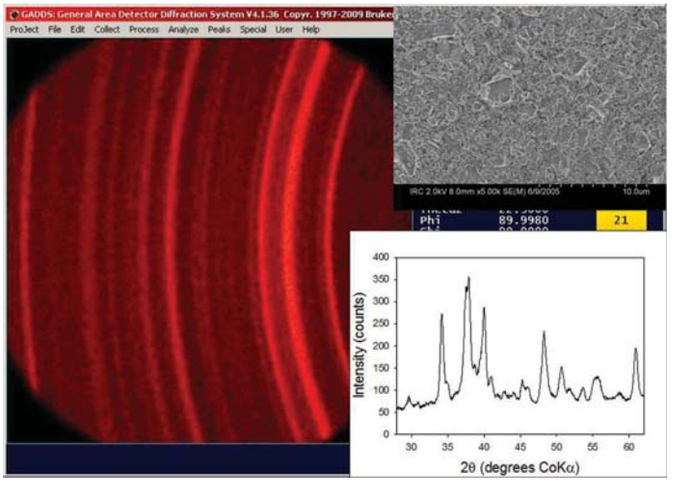

Figure 2.10.3
2D image from the same sample after reducing the crystallites down to a few µm, together with the properly averaged integrated data.

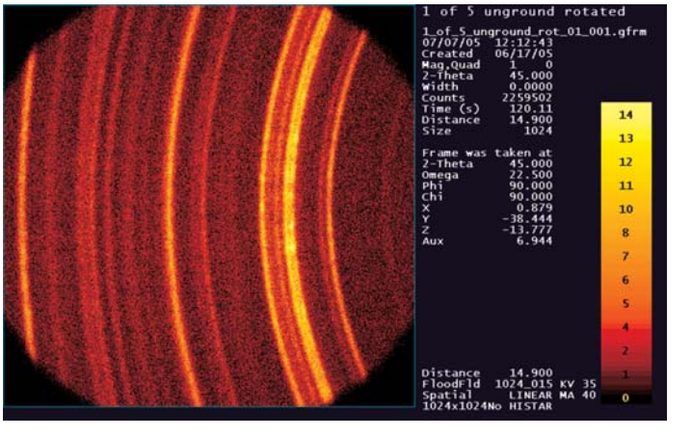

Figure 2.10.4
2D image showing the Debye rings when the unmilled sample from Fig. 2.10.2 is rotated. The slight spottiness shows that the quality is not as good as the milled sample, even when not rotated, as shown in Fig. 2.10.3.

typically very small beam divergence, and the tunable wavelength can be very helpful in circumventing some problems.

It will become apparent that many problems relating to specimen preparation and data quality are directly and indirectly the result of samples being too coarse to produce a random powder. The word 'powder' forms part of the name of the technique, but what makes a powder a powder?

2.10.1.1. *Powders and particle statistics (granularity)*

The question of when a powder is a 'true' powder is not new. It was dealt with in Klug & Alexander (1954) and Alexander & Klug (1948), and more recently by Smith (Smith, 2001; Buhrke *et al.*, 1998). The short answer is that at least 50 000 crystallites in the illuminated volume are necessary to obtain a random powder pattern.

The classic Debye rings of powder diffraction are formed by the random orientation of a large number of single crystallites, which are either physically separate or part of larger agglomerates. These rings used to be a common sight when film cameras were the norm, but can still be seen where two-dimensional (2D) or area detectors are used, most often on microdiffraction systems or synchrotron beamlines. Where there are sufficient crystallites diffracting, the spots from the crystallites merge into smooth rings. Problems with insufficient crystallites are often indicated by the presence of high-intensity spots in the Debye rings. When using 2D data sets, part or all of the intensity in the Debye rings may be integrated to produce an average 1D powder pattern.

More serious problems can arise in cases where 0D or 1D detectors are used. Most modern laboratory powder diffractometers use some form of 0D point detector (*e.g.* a scintillation counter) or 1D position-sensitive detector (PSD). When collecting data, these detectors pass through the Debye rings along a radius vector. Should the Debye ring be spotty, it is purely down to chance whether the detector will intersect with a spot of higher intensity or low intensity within the ring. An example of how spotty Debye rings can have an adverse effect on the integrated pattern can be seen in Fig. 2.10.2. Unfortunately there is usually no indication of the problem in the resulting integrated 1D pattern. The uncertainty with regard to the intensity of the Bragg reflections is something that must be minimized should accurate relative intensities be required for an analysis. This reproducibility is the concern when the term 'particle statistics' is used in relation to powder diffraction. The desirable smooth Debye rings shown in Fig. 2.10.3 were produced after reducing

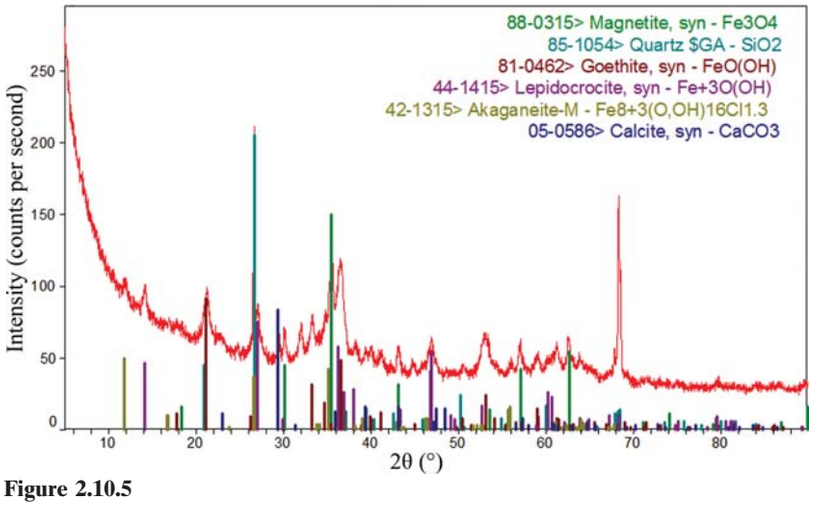

Figure 2.10.5
The appearance of specimen granularity in a hand-ground specimen of a railroad tank car corrosion deposit. The pattern was measured using a point detector. The intense sharp peak at ~68° 2θ turned out to come from a single crystal grain of sand at the surface of the specimen. The grain was detected by examination (after the measurement) in an optical microscope.

the crystallites to less than a few μm by milling. As shown in Fig. 2.10.4, rotating the coarse unmilled sample greatly improves the Debye rings compared with those seen in Fig. 2.10.2, but they are still not as uniform as those from the static milled sample in Fig. 2.10.3.

When using a point detector, granularity often manifests itself in the presence of a sharp (instrumental width) peak at relatively high diffraction angle. After a sharp peak at ~68° 2θ was observed in the pattern of a railroad tank car corrosion deposit (Fig. 2.10.5), examination of the specimen in an optical microscope indicated the presence of a single crystal grain of sand (quartz) on the surface. Re-grinding the specimen removed this artifact. Such sharp peaks tend to occur at relatively high diffraction angles, because at such angles the illuminated specimen area is smaller than at low angles, and the presence of a single crystal grain at the surface is relatively more important than when a larger area is illuminated.

An extreme example of granularity is provided by a hand-ground specimen of Scott's Moss Control Granules (Fig. 2.10.6). The even spacing of the strong peaks suggested severe preferred orientation, but examination of the specimen in an optical microscope (Fig. 2.10.7) revealed the presence of grains several tens of μm in size. Regrinding the sample in a McCrone micronizing mill reduced the crystallite size to a few μm (Fig. 2.10.7), and resulted in random powder data which could be used successfully in a Rietveld refinement (Fig. 2.10.8) and quantitative phase analysis.

An example of granularity at a synchrotron beamline is provided by $(Ba_{0.7}Sr_{1.3})TiO_4$ (Fig. 2.10.9). A Rietveld refinement using data collected from a static capillary specimen was unsuccessful. In an attempt to understand why, the diffractometer was driven to the 2θ angle of a strong peak, and a φ scan was carried out (rotating the capillary in steps). The intensity varied by a factor of five, as individual crystallites came into and out of diffracting position. Clearly, the intensities from such a measurement are not meaningful. When the capillary was rotated rapidly during a repeated φ scan, the intensity was constant and reliable.

Granularity can be encountered even in highly transparent organic specimens. A synchrotron pattern of 17α-estradiol showed that the sample was a mixture of the α-polymorph and an additional phase. Indexing the unknown peaks yielded the cell of the β-polymorph, the structure of which was unknown. The structure of the β-polymorph was solved using Monte Carlo simulated-annealing techniques, but the Rietveld refinement (Fig. 2.10.10) was not nearly as good as a Le Bail fit using the same cell and profile. The errors were then clearly in the structural model and/or the data. Examination of the specimen under an optical microscope revealed the presence of needles ~50 × 50 × 150–200 μm in size. Even the rapid rotation of the capillary specimen was not sufficient to obtain a powder average of such large crystallites.

Although granularity is normally considered to affect only the intensities of peaks, in extreme cases it can also affect the shapes. This is easily seen in a pattern from very coarse crystalline quartz in Fig. 2.10.11. The strange looking 101 reflection at 26.6° contains contributions from individual single crystals. When a wider view is taken, the relative intensities are distorted from those expected, similar to that seen in Fig. 2.10.2. Flat-plate data from highly-parallel-beam synchrotron beamlines are more (as opposed to less) susceptible, as shown by the comparison between flat-plate and capillary data of LaB_6 from the Australian Synchrotron in Fig. 2.10.12. Despite the use of ω-rocking and a Mythen position-sensitive detector, the flat-plate synchrotron data with 2–5 μm SRM660a LaB_6 crystallites show worse splitting of the Bragg peaks than lower-resolution laboratory data with 100 μm quartz crystallites.

The quantitative effect of particle statistics on diffraction results can be seen in Table 2.10.1. In the 15–50 μm sample the intensity varied from 4823 to 11 123 counts, which is a huge variation when trying to extract reliable intensities for analysis. Averaging over ten samples, the mean deviation was reduced from 18.2% to 1.2% when the smallest fraction of <5 μm was used. The absolute intensities of the largest fraction are significantly lower, which was attributed to extinction effects.

The source of this huge variation in errors can be understood more clearly when the theoretical treatment for quartz from

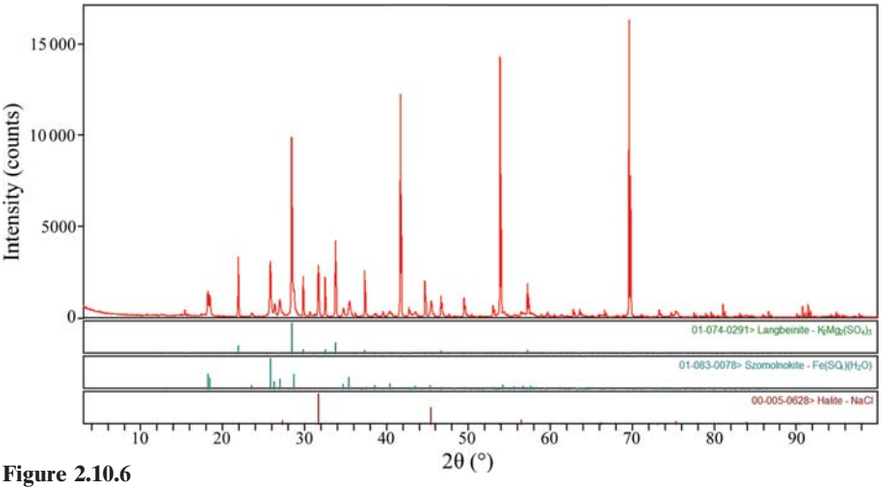

Figure 2.10.6
An extreme example of granularity. The pattern is of a hand-ground specimen of Scott's Moss Control Granules. No preferred orientation model could fit the langbeinite peaks.

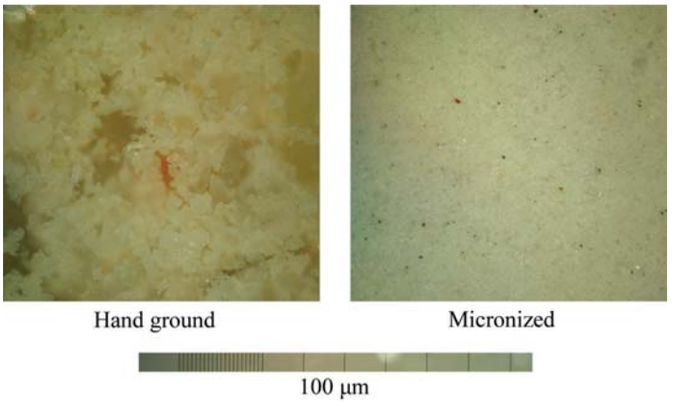

Figure 2.10.7
Optical microscope images of the surfaces of the hand-ground and micronized specimens of Scott's Moss Control Granules. The full length of the bar at the bottom is 100 µm. The hand-ground specimen contains grains much too large to yield a random powder pattern. Courtesy of B. J. Huggins, BP Analytical.

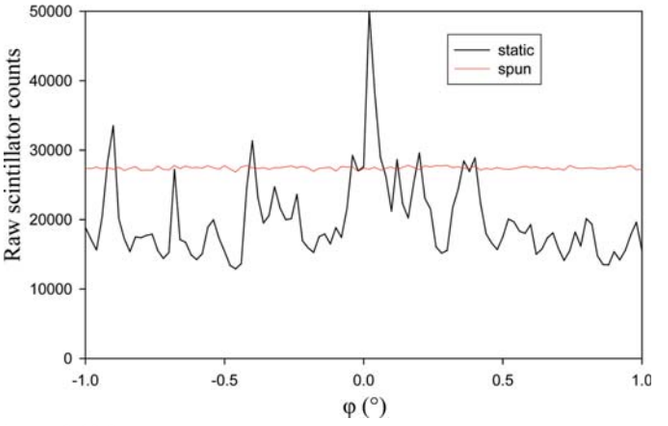

Figure 2.10.9
A rocking curve (φ scan) of $(Ba_{0.7}Sr_{1.3})TiO_4$, with the detector fixed at 9.647° 2θ, the top of a strong peak in the synchrotron pattern. The jagged plot is from a static specimen, and shows individual grains moving in and out of diffracting position. The flat curve is from a rotating specimen, and indicates that a powder average was obtained.

Smith (Smith, 2001; Buhrke *et al.*, 1998) is considered, which followed principles first described by de Wolff (1958). By considering the effects of crystallite size, illuminated volume and beam divergence, for a monodisperse 40 µm specimen Smith calculated that only 12 crystallites would be in the diffracting condition (assuming a point detector). Obviously this is nowhere near enough to create the desired smooth Debye rings. To obtain a standard error of less than 1% the number of diffracting crystallites should be over 52 900, which even the 1 µm sample fails to meet.

Why then does a powder diffraction experiment work? A number of factors may affect the effective number of crystallites, many of which will be mentioned in the following paragraphs. One that isn't is the multiplicity due to the crystal symmetry, meaning that there are always at least two equivalent orientations of each crystallite that would meet the diffraction condition, up to 48 for some cubic reflections. It is worth remembering that these figures relate to a single phase, so the impact on the errors in quantitative phase analysis can be considerable. For low-concentration phases, the number of crystallites is automatically smaller than those of the major phases, so the effects of granularity might be more pronounced.

When considering the granularity of a particular specimen there are a few things to consider. The number of diffracting crystallites depends on the illuminated volume (V), the size of the crystallites (s), the packing density (ρ) and the probability that a crystallite is in the correct orientation (P).

The illuminated volume V depends on a combination of instrument geometry, specimen geometry and the X-ray absorption of the sample. The footprint of the X-rays on a specimen in reflection depends on the beam width, beam length, the beam divergence (if any) and the diffraction angle. The effective beam width at the tube window with a typical long-fine-focus X-ray tube is 0.04 mm, with a length of 12 mm. The beam width may be increased up to 0.2 mm by using a broad-focus tube (Jenkins & Snyder, 1996), but these are rarely used in modern powder diffractometers. With Bragg–Brentano geometry the beam divergence may be increased to cover the available specimen, but large divergence angles degrade the peak resolution. A parallel-beam primary optic produces negligible beam divergence. The beam width may be reduced using an exit slit, but the largest beam width attainable is dependent on the characteristics of the mirror.

Additionally, V also depends on how deeply the X-rays can penetrate into the sample. This depends on the linear absorption coefficient of the specimen for the particular radiation being used, and is given (Klug & Alexander, 1954) by $t = (3.2\rho \sin\theta)/(\mu\rho')$, in which μ is the linear absorption coefficient, ρ is the crystal density and ρ' is the packing density. In the absence of other information, a reasonable assumption for the value of ρ'/ρ is 0.5. The penetration with Cu $K\alpha$ radiation can range from >1 mm for an organic material to a few µm for heavily absorbing specimens. With Bragg–Brentano geometry this leads to a potential trade-off between improving particle statistics and the peak shifts resulting from sample transparency. As a rule, doubling the diffracting volume will reduce the errors in intensity by about 1.5 times (Zevin &

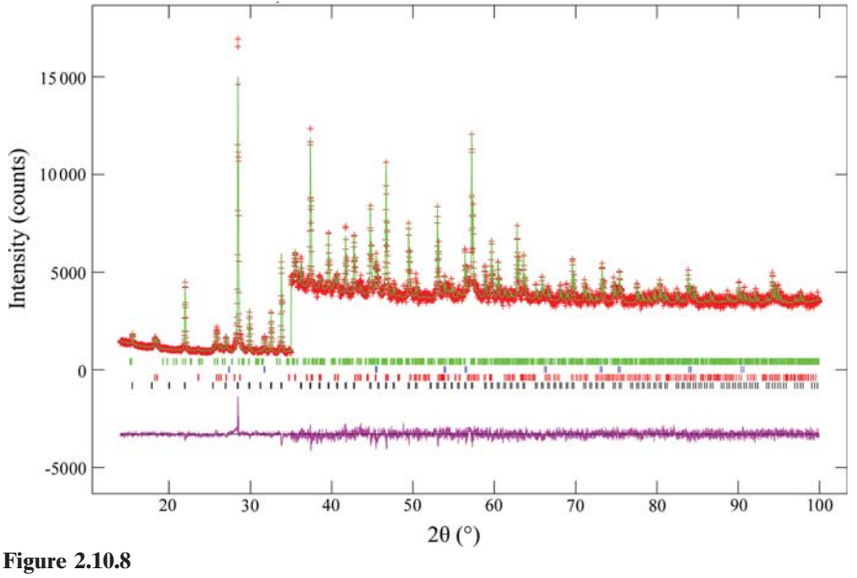

Figure 2.10.8
Rietveld refinement plot for micronized Scott's Moss Control Granules. No preferred orientation correction was necessary, and the specimen scattered as a random powder. For angles > 35° the vertical scale has been multipled by a factor of 5.

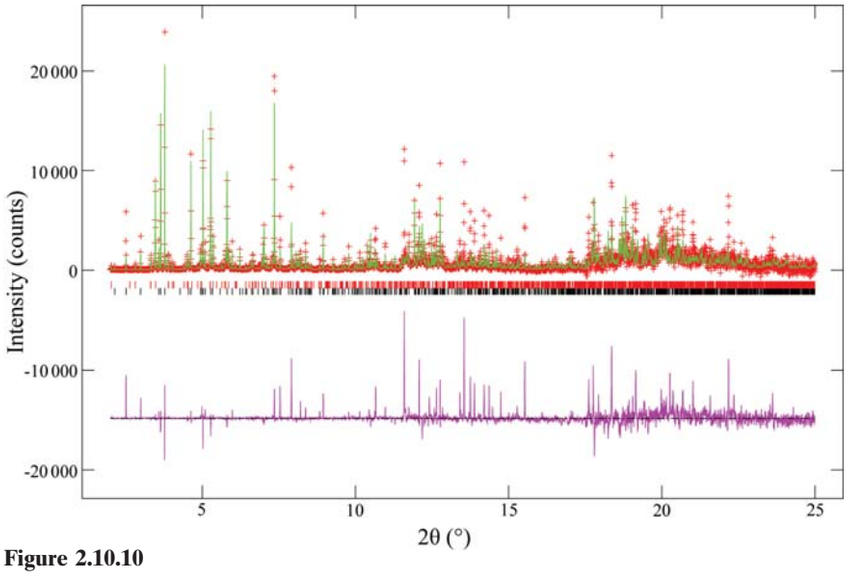

Figure 2.10.10
Rietveld plot of a mixture of β-17α-estradiol hemihydrate and α-17α-estradiol. The largest errors occur at the peaks of the β phase. Examination of the sample with an optical microscope revealed the presence of large single crystals. The rapid specimen rotation at the synchrotron beamline could not yield a powder average from such a coarse sample.

Kimmel, 1995), so is rarely sufficient on its own to solve problematic particle statistics.

Both the experimental data and theoretical treatment shown in Tables 2.10.1 and 2.10.2 show that with a typical laboratory setup, crystallites should ideally be in the range of a few μm in size to produce accurate intensity data. Reducing the crystallites to below 1 μm will improve the statistics further but may also induce crystallite-size and/or microstrain broadening depending on the instrument resolution. It is important to note that the crystallites must be uniformly small. Mineralogists often refer to 'rocks in dust', where there are a small number of very large crystallites scattered among the sample. Scattering of X-rays is sensitive to statistics by *volume*. A few very large crystallites will dominate (and probably distort) the resulting pattern, so the 'rocks in dust' scenario should be avoided whenever possible by correct specimen-preparation techniques.

As we have seen previously, the granularity can be seen visually in a 2D data set. If the researcher has access to a 2D detector this is the quickest way to assess a sample. However, where such a system is not available, an alternative is to use φ scans. In simple terms this involves taking data sets of a static specimen but rotating the specimen by a particular angle between data sets, for example at 0, 90, 180 and 270° in φ. Ideally the patterns should overlap exactly, although in practice one is looking for reproducible relative intensities, as the absolute intensities may change slightly. The examples used here are the so-called 'five fingers' of quartz. Although they are relatively weak reflections in the quartz pattern, three overlapping $K\alpha_{1,2}$ doublets provide a conveniently compact example. The three data sets shown in Fig. 2.10.13 are -400-mesh quartz (<38 μm), a commercial quartz with a size less than 15 μm and a sample milled to less than 5 μm. Optical micrographs of the -400 mesh and milled quartz samples are shown in Fig. 2.10.14.

The most obvious feature of the φ scans is that the reproducibility of the relative intensities is poor with the -400 mesh quartz sample. This has obvious consequences for any analytical technique relying on accurate peak intensities. All eight of the patterns from the micronized sample have practically identical relative peak intensities. It is worth comparing the similar results in the variability visible in Fig. 2.10.13 with the tabulated errors for the different methodology used for the data in Table 2.10.1.

The final approach to improving statistics is to increase the probability P that a crystallite is in the diffracting condition and visible to the detector. The latter is relevant today with 1D PSD detectors becoming more common, as the detector can simultaneously see multiple crystallite orientations at a particular incident beam angle, as shown in Fig. 2.10.15. P also increases with beam divergence; although there are many advantages of parallel-beam geometry, improving particle statistics is not one of them.

P is much higher with capillary transmission geometry than for reflection geometry. By rotating the specimen about an axis normal to the beam the effective number of orientations 'seen' by the detector increases greatly. This is the reason why a powder passing a 325-mesh sieve (<45 μm) almost always yields smooth

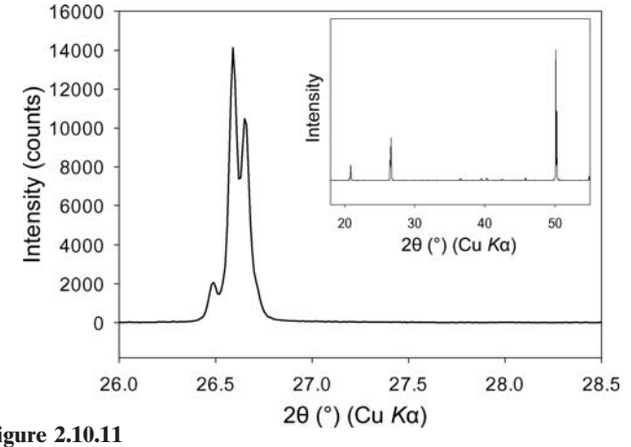

Figure 2.10.11
The main 101 reflection in data collected from a very coarse (~100 μm) highly crystalline quartz. The strange peak splitting is characteristic where there are very large crystallites present in the sample. The inset shows the diffraction pattern over a wider range and the strangely high intensity at 50° 2θ is caused by the detector intersecting a very intense diffraction spot similar to that seen in the lower part of Fig. 2.10.2.

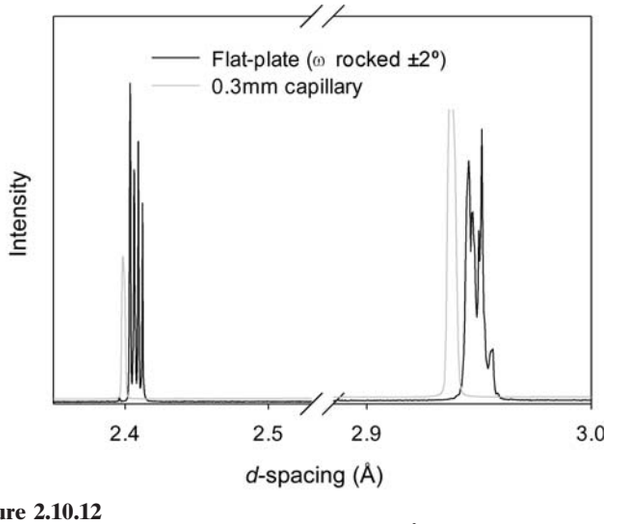

Figure 2.10.12
Comparison between capillary (0.3 mm, 0.8265 Å) and rocking flat-plate (strip heater, 1.2386 Å, ω ±2°) data from the Australian Synchrotron. Data courtesy of Ian Madsen, CSIRO.

Table 2.10.1
Intensity (counts) and mean deviation in intensity of the main quartz 101 reflection with a stationary sample of -325 mesh quartz powder

Data from Alexander *et al.* (1948) and Klug & Alexander (1954).

	Crystallite size			
Data set	15–50 μm	5–50 μm	5–15 μm	<5 μm
1	7612	8688	10841	11055
2	8373	9040	11336	11040
3	8255	10232	11046	11386
4	9333	9333	11597	11212
5	4823	8530	11541	11460
6	11123	8617	11336	11260
7	11051	11598	11686	11241
8	5773	7818	11288	11428
9	8527	8021	11126	11406
10	10255	10190	10878	11444
Mean % deviation	18.2	10.1	2.1	1.2

Table 2.10.2
Theoretical behaviour of different crystallite sizes of quartz in a volume of 20 mm^3

Data from Smith (2001).

Crystallite diameter (μm)	40	10	1
Crystallites per 20 mm^3	5.97×10^5	3.82×10^7	3.82×10^{10}
No. of diffracting crystallites	12	760	38 000

Debye rings in a capillary (Klug & Alexander, 1954), while the pattern would be granular in reflection. Specimen rotation has also been long employed in reflection geometry (de Wolff, 1958; de Wolff *et al.*, 1959), and a sample spinner is now a standard attachment for commercial diffractometers. When properly applied, the use of a spinner can reduce the standard deviation of the integrated intensity by a factor of approximately 4–5 (~7–8 for peak intensities) (de Wolff *et al.*, 1959), corresponding to a reduction in the effective crystallite size by a factor of 3 (Zevin & Kimmel, 1995). However, depending on the sample, as seen in Table 2.10.2 this can be insufficient on its own as it rotates the specimen only in a single plane. Where a spinner is used in conjunction with a point counter, it is important that the spinner must complete at least one rotation during each step to maximize its effectiveness. In order to further improve the particle statistics it is possible to construct spinners that tilt back and forth along an axis normal to the beam (similar to the capillary concept) in addition to the normal axis of rotation. This is effective in improving particle statistics but adversely affects the para-focusing condition in Bragg–Brentano geometry. It is important to note that specimen rotation improves grain-sampling statistics, but does nothing to alter preferred orientation.

The term 'micronized' is one that is frequently seen in papers on quantitative phase analysis. Potentially any kind of mill could be used to reduce the crystallites down to the desirable μm size range (such as shown in Fig. 2.10.14*a* and *b*). However, most mills use high-energy percussion-like impacts between the grinding media and the sample, which tend to damage the crystal structure in softer materials and induce microstrain into the material. In extreme cases the sample can become completely amorphous. There is also the potential problem of modifying the polymorph with samples susceptible to such changes. The mill produced by McCrone (http://www.mccrone.com) was designed specifically for the preparation of X-ray diffraction and X-ray fluorescence samples, and the shearing milling mechanism minimizes damage *versus* conventional impact milling. It is necessary to use wet milling to produce the best results, so it is up to the analyst to

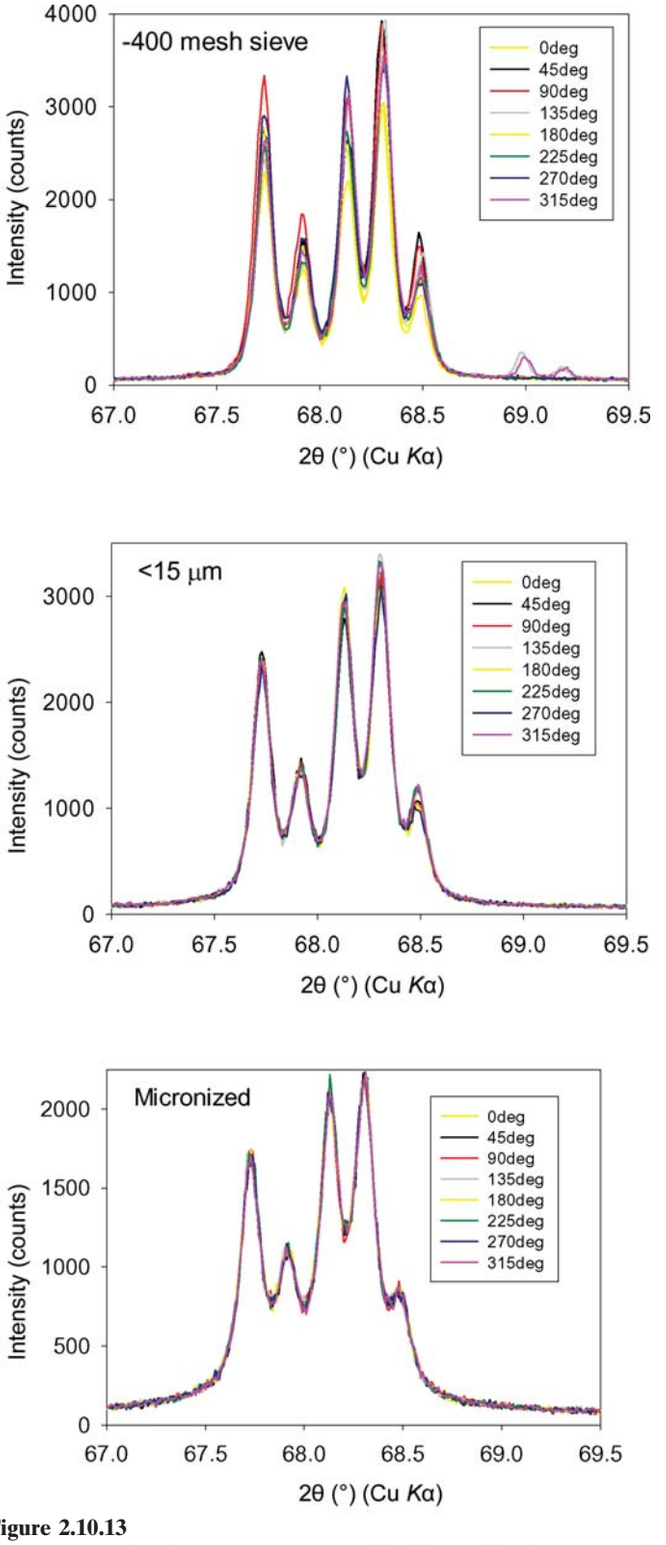

Figure 2.10.13
φ scans of the five fingers of quartz for (*a*) <38 μm, (*b*) <15 μm and (*c*) micronized samples.

choose the best media compatible with both the sample and the polymer micronizing vials. Commonly used are ethanol, isopropyl alcohol, *n*-hexane and water; it is not advisable to use acetone, as this solvent dissolves the polymer jars supplied with this mill. A limitation of most forms of milling is the requirement for a relatively large amount of sample. In the McCrone mill a volume of >1 ml is usually required, although desperate scientists have been known to dilute the specimen with amorphous material, such as silica gel. The analyst should also be aware of the possible contamination of samples by degrading and eroding grinding

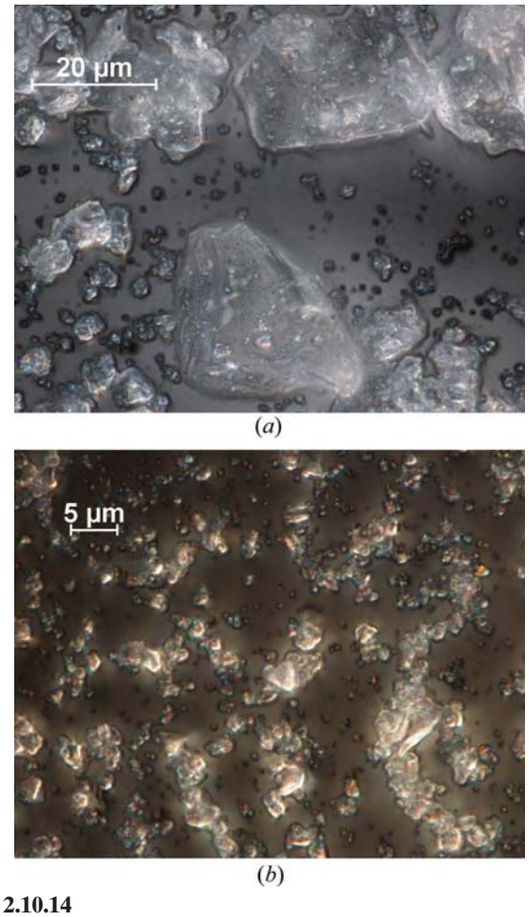

Figure 2.10.14
Optical micrographs of (*a*) -400 mesh quartz at 100× magnification and (*b*) quartz milled in a McCrone micronizer for 15 min in isopropyl alcohol at 150× magnification.

elements (corundum or agate in the micronizing mill; possibly iron, WC, SiC *etc*. in other types of mill).

Obviously, a reduction of the crystallite size to the μm-sized region will produce size broadening if the instrument has sufficient resolution to detect it. It is worth bearing in mind that micronizing does not guarantee a problem-free sample. Micronized specimens almost always exhibit some microstrain broadening. In principle, this could be decreased by an annealing treatment, but this step is rarely practiced. When a mixture contains both very hard and very soft phases, the hard phases may not mill properly. This has been observed in mixtures containing organics and a minor quartz fraction. Despite milling for 30 min or more, the classical split 101 quartz reflection (such as seen in Fig. 2.10.11) was still visible in some data sets, an indication of the 'rocks in dust' phenomenon. Although the McCrone mill is designed to minimize microstructural damage to samples, damage can still occur with very soft materials, and ductile materials may weld as opposed to mill. With very soft and pliable materials a possible alternative could be to cryo-mill the samples, taking advantage of the increased brittleness of materials at low temperature.

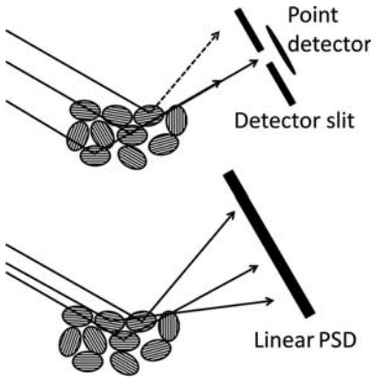

Figure 2.10.15
Diagram showing the source of improved particle statistics in reflection geometry using a 1D position sensitive detector (PSD) *versus* a point detector.

2.10.1.2. *Preferred orientation*

Preferred orientation is usually undesirable in a powder diffraction pattern, although sometimes it *is* the information required, as in texture studies. One of the exceptions is the analysis of clays, where orientation is deliberately induced to identify related reflections. Preferred orientation manifests itself as continuous but non-uniform intensity in the Debye rings, and so is easily characterized with 2D detectors. Preferred orientation does not change the total diffracted intensity, but renormalizes some classes of reflections with respect to others.

Reference is commonly made to a preferred-orientation 'correction'. Strictly speaking, what is done is 'modelling' of the preferred orientation. The proper way to correct preferred orientation is through better specimen preparation.

Models for preferred orientation exist in many analysis packages, specifically the March–Dollase (Dollase, 1986) and spherical-harmonics (Järvinen, 1993) formalisms. Apparent severe preferred orientation may be a sign of large crystallites, which may result in one or more of the other problems outlined in this section.

Additional care must be taken where software corrections are used during quantitative phase analysis, where overlapping reflections can cause serious correlations and erroneous results. The March–Dollase correction is less prone to this, as an orientation direction must be supplied by the analyst. The spherical-harmonics correction has no such constraint. It behaves properly where peak overlap is not extensive, but negative peak intensities are not uncommon (especially when too high an order is used) when applying it without thought in complex mixtures. Negative peak intensities are obviously impossible, so the results of such an analysis must be viewed with great suspicion.

The presence of preferred orientation can be most easily discerned by comparing the observed pattern to a calculated pattern (random) of the same phase from the Powder Diffraction File or other source. The likelihood of preferred orientation can be assessed by calculating the Bravais–Friedel–Donnay–Harker (Bravais, 1866; Friedel, 1907; Donnay & Harker, 1937) morphology from the crystal structure using *Mercury* (Sykes *et al.*, 2011) or other tools.

Orientation tends to occur in materials where the crystallites have either a needle or plate-like morphology. Plates are common in the analysis of mineral samples, such as the commercial phlogopite mica used here as an example. Conventional top-loading of such samples can result in very few reflections being visible because of almost perfect orientation of the plates during pressing, as seen in Fig. 2.10.16. Where the aspect ratio of the crystallites is large, micronizing the sample does not reduce the preferred orientation significantly (Fig. 2.10.17).

The most common approach to decrease preferred orientation of troublesome samples such as this mica is a technique known as back-loading. [Others are discussed in Buhrke *et al.* (1998).] The concept is that the surface of the sample is not subjected to